Journal of Catalysis **186,** 269–278 (1999)
Article ID jcat.1999.2518, available online at http://www.idealibrary.com on IDEAL®

Decomposition of Ethane and Its Reaction with CO_2 over Rh/ZSM-5 Catalyst

Frigyes Solymosi, Attila Szõke, and László Ovári

Institute of Solid State and Radiochemistry, Attila József University and Reaction Kinetics Research Group of the Hungarian Academy of Sciences,[1] P.O. Box 168, H-6701 Szeged, Hungary

Received December 18, 1998; accepted April 13, 1999

The interaction of ethane with Rh/ZSM-5 and its decomposition and reactions with CO_2 on Rh/ZSM-5 have been investigated. Methods used were Fourier-transform infrared spectroscopy and temperature-programmed desorption and reaction (TPD and TPR). The decomposition of ethane and its reaction with CO_2 have been studied in a fixed-bed continuous-flow reactor. IR measurements showed that ethane interacted strongly with the highly dispersed Rh above 206 K and gave rise to the formation of ethylidyne surface species very likely through the transient formation of ethylene. At 523–573 K, the decomposition of ethane produces hydrogen, methane, and propane. Above 623 K ethylene became the main product, but benzene and toluene were also detected. Independent of the temperature, the rate of the decomposition decayed after 5–10 min to a very low level (1–2% conversion), but it did not cease completely even after several hours (673 K). The reactivities of surface carbon formed at different temperatures toward H_2, O_2, and CO_2 have been examined. Carbon exhibited the highest reactivity with O_2 and less reactivity with CO_2. The peak temperatures of its reaction in TPR shifted to a higher temperature with the temperature of its production in all the three cases. Carbon formed at 773 K in the ethane decomposition reacted with CO_2 at maximum rate at 973 K. The reaction between C_2H_6 and CO_2 occurred rapidly above 700 K to give mainly H_2 and CO with a ratio of 0.3–0.6. In contrast with the $CH_4 + CO_2$ reaction on the same catalyst, a significant deactivation of the catalyst occurred at the stoichiometric CO_2/C_2H_6 ratio. This feature is attributed to the low reactivity of hydrocarbon fragments formed by the decomposition of ethane compared to those produced by CH_4 dissociation. Deactivation can be decreased or almost ceased by using a large excess of CO_2. © 1999 Academic Press

Key Words: **adsorption of ethane; decomposition of ethane; formation of ethylidyne from ethane; Rh/ZSM-5 catalyst; FTIR spectroscopy; reactivity of surface carbon; dissociation of CO_2; reactions of ethane with CO_2; production of synthesis gas; deactivation of Rh/ZSM-5.**

1. INTRODUCTION

Utilization of cheap raw materials, such as CH_4 and CO_2, requires considerable effort (1, 2). After extensive research on the oxidative coupling of methane (1, 2), attention turned to the conversion of methane into higher hydrocarbons under nonoxidative conditions. Supported Rh was found to be an effective catalyst for the decomposition of methane and in the hydrogenation of carbonaceous material formed into saturated and unsaturated hydrocarbons (3–7). Although the formation of higher C_xH_y can be increased by adding Cu promotor to the Rh (7), the conversion of methane into other C_xH_y compounds is still very low. A more efficient catalyst for CH_4 conversion is MoO_3 deposited on ZSM-5 (8, 9). It can convert methane into benzene with 70–80% selectivity at 7–10% conversion at 973 K (8–15). The catalytic reaction is preceded by an induction period during which MoO_3 is reduced and a large amount of carbon is deposited (10). This observation led to the assumption that Mo_2C formed with process was an actual catalyst for the methane activation (11–15). The same behavior was observed in the aromatization of ethane on MoO_3/ZSM-5 and Mo_2C/ZSM-5 (16).

An alternative way to utilize both CH_4 and CO_2 is through their reaction, which produces synthesis gas $CO + H_2$ (17, 18). Supported Ni is an active catalyst for this process, but its rapid deactivation due to coking causes a serious problem, and several attempts have been made to avoid the carbon deposition (17–20). However, no or only a slight deactivation was observed for rhodium, which also exhibited high activity (6, 21–27).

As the natural gas may contain a small amount of ethane, recently we examined its effects on the CH_4–CO_2 reaction over Rh/ZSM-5 (28). We found that the presence of ethane strongly deactivated the catalyst and caused the enhancement of carbon deposition (28). The primary aim of this study is to elaborate this effect. For this purpose we examine the interaction and decomposition of ethane on Rh/ZSM-5 and its reaction with CO_2 at low and high temperatures. There are relatively few works devoted to the $C_2H_6 + CO_2$ reaction (29, 30). They dealt only with the oxidative dehydrogenation and aromatization of C_2H_6 using CO_2 as oxidant. Greater attention was paid, however, to the steam reforming of ethane on Ni-based catalysts (31, 32).

---

[1] This laboratory is a part of the Center for Catalysis, Surface and Material Science at József Attila University of Szeged.

0021-9517/99 $30.00

2. EXPERIMENTAL

The catalysts were prepared by impregnating H-ZSM-5 (Si/Al = 55) with $RhCl_3 \cdot 3H_2O$ salt to yield a nominal 2 wt% metal. The catalyst samples were oxidized at 573 K for 30 min and reduced at 773 K for 60 min. The dispersion of Rh, determined by H_2 adsorption at 300 K, is 9.2%. The gases used were initially of commercial purity. CO_2 was further purified by fractional distillation. He (99.995%) and Ar (99.995%) were used as received. Catalytic measurements were carried out in a fixed bed continuous flow reactor made of a quartz tube. In the case of C_2H_6 decomposition the carrier gas was Ar which contained 12.5% of C_2H_6. In the kinetic study of $CO_2 + C_2H_6$ reaction we used a gas mixture of 6 : 1 mole ratio without Ar. The amounts of catalyst were 0.3 g (C_2H_6 decomposition) and 0.5 g ($CO_2 + C_2H_6$ reaction). The space velocity (total) was in general 6000 h^{-1}. Inert gas was used as diluent to determine the partial order of carbon monoxide and hydrogen formation. The exit gases were analyzed gas chromatographically (Hewlett–Packard 5890) on a Porapak QS column. For IR spectroscopic experiments the powdered material was pressed into 10 × 30-mm self-supporting disks. Infrared spectra were recorded with a Bio-Rad Fourier transform IR spectrometer (FTS 155) with a wavenumber accuracy of ±4 cm^{-1}. Typically 136 scans were collected. Supplementary methods used were temperature-programmed desorption (TPD) and temperature-programmed reaction (TPR). The heating rate was 12 ml/min.

3. RESULTS

3.1. *Interaction of C_2H_6 with Rh/ZSM-5*

To identify the surface species formed during the interaction of ethane with the Rh/ZSM-5 catalyst, detailed IR spectroscopic measurements were performed. In the first experiments the following approach was used: 10 Torr of ethane was contacted with the reduced catalyst for 10 min at 300 K, then the cell was degassed, and spectra were registered as a function of temperature. We observed a relatively intense absorption band at 1342 cm^{-1} and much weaker ones at 2800 and 2879 cm^{-1}. The intensities of these bands decreased with increasing annealing temperatures, and the bands were not detectable above 423 K. The tentative assignment of these bands suggests that adsorbed ethane underwent a partial dehydrogenation at 300 K and the ethylidyne surface species was produced (see Table 1 and Discussion).

To establish the lowest temperature in this process, ethane adsorption was performed at ∼146 K, and the sample was warmed under continuous evacuation. Absorption bands were observed at 2969, 2940, 2918, 2881, 1445, and 1371 cm^{-1} (Fig. 1A). With increasing temperature all the bands attenuated and finally disppeared above 206–225 K. At 206 K, however, a weak new band developed at 1342 cm^{-1}. In the next experimental series the reduced Rh/ZSM-5 catalyst was exposed to 10 Torr of ethane at different temperatures, and after degassing the IR spectra were registered. Some select spectra are presented in Fig. 1B. It shows that the intensity of the 1342 cm^{-1} band gradually increases with the adsorption temperature up to 300 K. At this temperature weak bands at 2849 and 2800 cm^{-1} were also detected (not shown in the spectra). Attenuation of all these bands occurred above room temperature.

Similar measurements were carried out with Rh-free support. Adsorption of ethane on ZSM-5 at 300 K produced no stable absorption bands that survived the evacuation at room temperature. Lowering the adsorption temperature to 146 K, we obtained absorption bands the same as

TABLE 1

Vibrational Frequencies following C_2H_6 Adsorption and Their Assignments

C_2H_6				CCH_3		
Assignment	C_2H_6 gas (33)	C_2H_6/ZrO_2 (34)	C_2H_6/ZSM-5 present study[b]	Assignment	Pt/SiO_2 (43)[c]	Rh/ZSM-5 present study[c]
$\nu_a(CH_3)$	2985	2974	2969	$\nu_a(CH_3)$	—	
$\nu_a(CH_3)$	2969[a]	2953	2940	$\nu_s(CH_3)$	2879	2879
$\nu_s(CH_3)$	2954[a]	2916	2918	$2\delta_a(CH_3)$	2795	2800
$\nu_s(CH_3)$	2896	2884	2881	$\delta_a(CH_3)$	—	
$2\delta_a(CH_3)$				$\delta_s(CH_3)$	1348	1342
$\delta_a(CH_3)$	1469	1464	1445			
$\delta_a(CH_3)$	1468[a]	(1514)	—			
$\delta_s(CH_3)$	1338[a]	—	—			
$\delta_s(CH_3)$	1379	(1340)	1371			
$\rho(CH_3)$	1190[a]	(1173)				

[a] Not IR active.

[b] Temperature, 146–186 K.

[c] Temperature, 293 K.

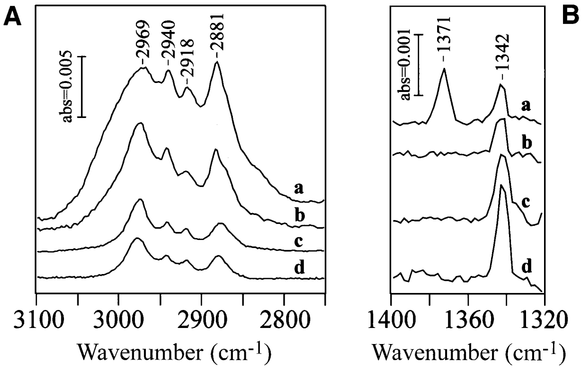

FIG. 1. (A) Infrared spectra following C_2H_6 adsorption (10 Torr) and subsequent evacuation on ZSM-5 at (a)140 K and (b)186 K and on Rh/ZSM-5 at (c) 140 K and (d) 206 K. (B) Effects of the adsorption temperature of ethane on the peak at 1342 cm^{-1}: (a) 206 K, (b) 225 K, (c) 273 K, (d) 293 K.

those registered for Rh/ZSM-5. Annealing the adsorbed layer caused the elimination of all bands around 206 K, without producing any new spectral feature. Some spectra obtained are displayed in Fig. 1A.

TPD and TPR measurements showed that following the adsorption of ethane at 373 K, the release of methane was observed with $T_p = 460$ K. An evolution of ethane also occurred, indicating that a certain amount of ethane was not removed during purging of the sample with argon after adsorption. A significant hydrogen desorption ($T_p = 620$ and 850 K) was observed after 523 K adsorption along with a small amount of methane desorption ($T_p = 650$ K). The desorbed amount of both compounds increased with the increase in adsorption temperature up to 623 K. In this case the T_p for CH_4 was 700 K and the T_p's for H_2 were 680 and 890 K. Some TPR curves are displayed in Fig. 2.

3.2. Decomposition of C_2H_6 in a Flow System

The formation of gaseous products in the decomposition of C_2H_6 on Rh/ZSM-5 was observed even at 523 K, where the initial conversion was 0.8%. The products were H_2, CH_4, C_2H_4, and C_3H_8. At and above 573 K a small amount of C_6H_6 was also formed. With the increase in temperature, the extent of the decomposition significantly increased: the initial decomposition was 3.1% at 673 K and 24.0% at 773 K (Fig. 3A). The conversion of ethane, however, markedly decayed in time, very likely due to carbon deposition. Figures 3B and 3C show the effect of temperature on the yields of various compounds. The yields of hydrocarbons formed varied with the increase in temperature. The largest enhancement was observed for ethylene. The yield of benzene remained low, below 5%, in the range of 623–773 K.

With regard to the effect of flow rate we found that the lower the flow rate the higher the conversion. Variation of the C_2H_6 content in the gas mixture also exerted a significant influence on the rates of production of C_2H_4 and H_2. In pure C_2H_6, the H_2 formation rate was more than five times higher than that for the gas mixture containing 12.5% C_2H_6.

Note that on Rh-free ZSM-5 no reaction of ethane was experienced below 773 K. Above this temperature ZSM-5 exhibited a significant activity toward the conversion of ethane into higher hydrocarbons and benzene.

3.3. Formation and Reactivity of Surface Carbon

The reactivity of carbon with H_2, CO_2, and O_2 produced by the decomposition of ethane on Rh/ZSM-5 was

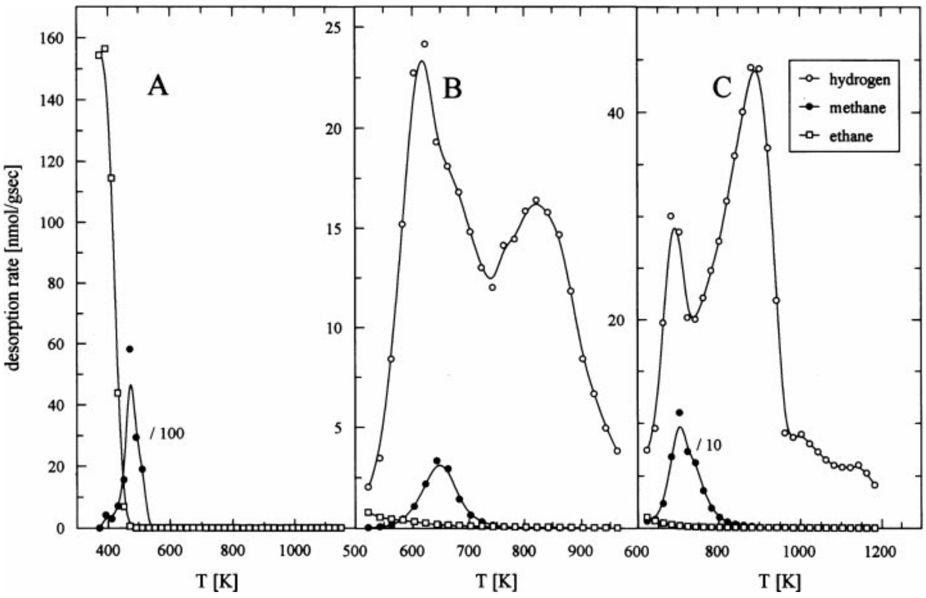

FIG. 2. TPR measurements following C_2H_6 adsorption on Rh/ZSM-5 at different temperatures. The adsorption temperatures were (A) 373 K, (B) 523 K, and (C) 623 K.

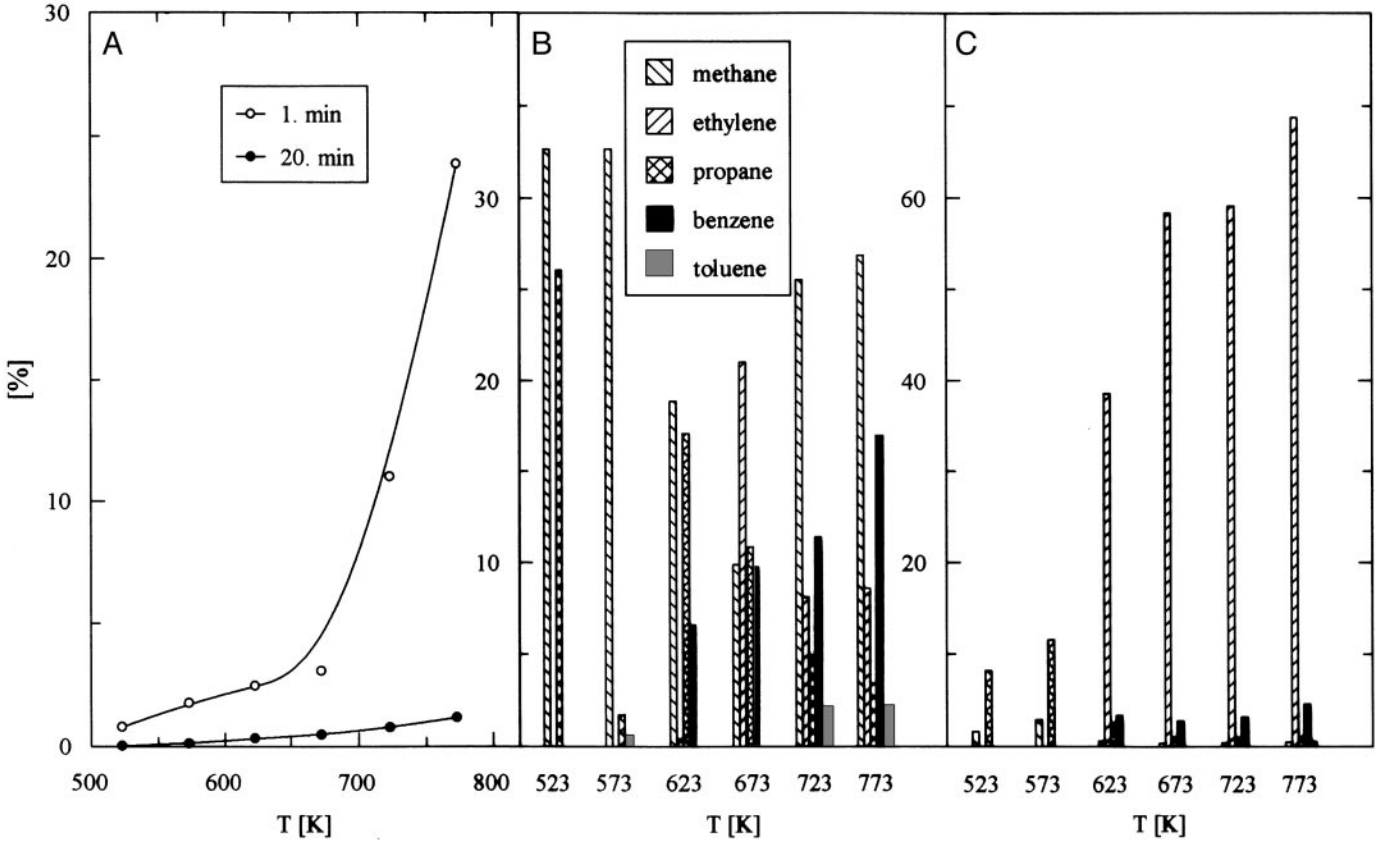

FIG. 3. Conversion of ethane (A) and the yield of various products formed in the decomposition of ethane on Rh/ZSM-5 at different temperatures at 1 min (B) and 20 min (C). The flow rate was 12 ml/min. Data were obtained on fresh catalyst, at every temperature.

examined. The carbon formed at 773 K exhibited very low reactivity. Its oxidation started at the lowest temperature, above 473 K. The peak temperature was ∼700 K. The hydrogenation of this carbon began at a much higher temperature, above 700 K, with $T_p = 820$ and 900 K. The reaction of carbon with CO_2 also occurred in this temperature range with $T_p = 973$ K. The corresponding TPR spectra are displayed in Fig. 4A. When the carbon was produced at low temperature, 623 K, all the T_p values shifted to lower temperatures. The results are shown in Fig. 4B. The reactivity of surface carbon with CO_2 produced at 623 K was also examined. However, we could not detect any reaction in the low temperature range. The formation of gaseous CO was observed only at 620 K, and the highest rate was measured at 805 K (Fig. 4B). As CO desorbed from Rh above 450–500 K, there was a possibility that C would react with CO_2 even at a lower temperature, but the CO formed remained adsorbed on Rh. IR spectroscopic studies, however, did not support this idea: a CO band was not detected.

In separate experiments we determined the other products formed in the hydrogenation of carbonaceous species (produced by ethane decomposition) by using H_2 pulses. Following the ethane adsorption at 523 K, we detected very small amounts of propane and benzene, in addition to methane and ethane. Their amounts gradually decreased with the temperature of ethane decomposition. At $T_a = 773$ K they were completely missing from the reaction products, and we measured only methane and ethane. Some results are listed in Table 2.

3.4. Interaction of $C_2H_6 + CO_2$ Gas Mixture on Rh Catalyst

The most sensitive method for following the interaction of CO_2 with H-containing compounds over supported Rh is IR spectroscopy, as CO, the primary product of this surface process, is strongly bonded to the Rh (6). In the absence of ethane, FTIR spectroscopy revealed no dissociation of CO_2 on Rh-ZSM-5 catalyst up to 573 K. Note that adsorbing

TABLE 2

Formation of Hydrocarbons (in μmol/g) in the Reaction at Eight Hydrogen Pulses with Carbonaceous Compounds Produced by the Decomposition of Ethane on Rh/ZSM-5 at 523 K for 2 min

	CH_4	C_2H_6	C_3H_8	C_6H_6
523 K	221.3	4.41	0.123	0.082

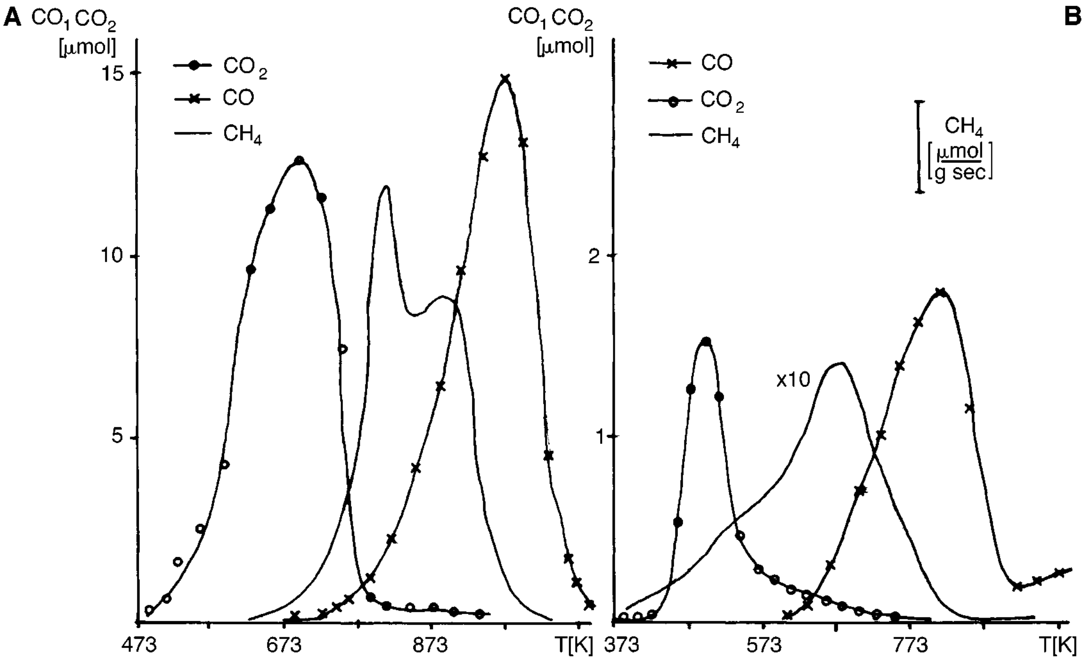

FIG. 4. Temperature-programmed reactions of surface carbon with H_2 (—) (the product is CH_4), O_2 (×) (the product is CO_2), and CO_2 (○) (the product is CO). Carbon was produced in the decomposition of C_2H_6 on Rh/ZSM-5 at 773 K for 1.5 min (A) and at 623 K for 20 min (B).

CO on the 2 wt% Rh/ZSM-5 catalyst, reduced at 773 K, gave an intense band at 2065-2075 cm^{-1}, and a weak one at 1830 cm^{-1}, but there was no indication of the development of the dicarbonyl species in 150 min.

Following the coadsorption of the $CO_2:C_2H_6$ (4:1) gas mixture (20 Torr) from 240 to 300 K, we observed no spectral changes indicative of the dissociation of CO_2. In addition, CO_2 did not exert an appreciable influence on the spectral features detected after C_2H_6 adsorption (Fig. 1). At and above 523 K, however, a weak absorpion band developed at 2030 cm^{-1}, which gained intensity with the increase in the adsorption time (Fig. 5). This band undoubtedly belongs to CO linearly bonded to the Rh cluster. With the increase in the temperature of the gas mixture, the intensity of the CO band gradually enhanced and slightly shifted to lower frequencies, to 2024 cm^{-1}. At the same time another linearly bonded CO, absorbing at 2050 cm^{-1}, and a bridge bonded CO, absorbing at 1850 cm^{-1}, developed.

3.5. $C_2H_6 + CO_2$ Reaction

Similarly, as observed for the $CH_4 + CO_2$ system, the addition of a small amount of CO_2 (5–10% of C_2H_6) to C_2H_6 exerted no influence on the decomposition of C_2H_6 at low temperatures, 523–573 K. However, at higher temperatures, the reaction pathway changed: the formation of C_2H_4 ceased and CO appeared among the products. The formation of methane, however, still occurred.

The $C_2H_6 + CO_2$ reaction to produce synthesis gas was studied in the temperature range 700–773 K. The performance of the catalyst sensitively depended on the $CO_2 + C_2H_6$ mole ratio (Fig. 6A). Even in the case of a stoichiometric gas mixture ($CO_2/C_2H_6 = 2.0$), the catalyst rapidly lost its activity. The rate of the deactivation decreased with the increase in CO_2 content, and in the presence of a large excess of CO_2 (CO_2/CH_4 4), no activity decrease was experienced during the measuring time, 24 h. The amount of carbon deposited during a 2-h reaction at 773 K was determined by TPR measurement (Fig. 6B). While in a stoichiometric gas mixture 185.4 μmol/g formed, this value decreased to 69.7 μmol/g at $CO_2/C_2H_6 = 4$ and to 9.38 μmol/g at $CO_2/C_2H_6 = 6$.

In Table 3 we present the product ratios at different compositions of reacting gas mixture. The H_2/CO and the H_2/CH_4 ratios varied between 0.27 and 0.37 and 0.5 and 0.77,

TABLE 3

The Product Ratios of $CO_2 + C_2H_6$ Reaction on Rh/ZSM-5 at Different Compositions of Reacting Gases at 773 K

CO_2/C_2H_6 ratio	H_2/CO	H_2/CH_4	CO/CH_4
2:1[a]	0.33	0.35	1.02
2:1[b]	0.90	(33.0)	(~30.0)
4:1	0.37	0.55	1.50
8:1	0.31	0.59	1.81
12:1	0.27	0.77	2.70

Note. The C_2H_6 content of gas mixture was kept constant, 5.2%.
[a] Measured at 1 min.
[b] Measured at 60 min.

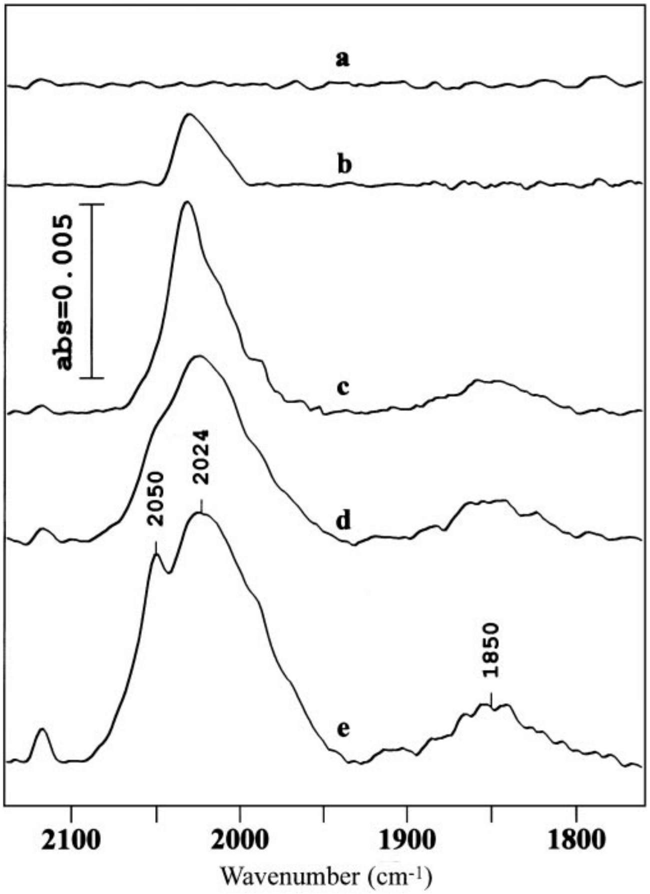

FIG. 5. Infrared spectra of Rh/ZSM-5 following the adsorption of the $C_2H_6 + CO_2$ gas mixture at different temperatures. (a) 300 K, (b) 523 K for 5 min, (c) 523 K for 60 min (d) 573 K for 5 min, (e) 573 K for 60 min.

respectively. Somewhat different values were obtained for the stoichiometric composition, very likely due to the rapid deactivation.

Lowering the reaction temperature led to an increase in the H_2/CO ratio and to a decrease in the CO/CH_4 and H_2/CH_4 ratios. At 723 K, a slow deactivation was experienced even in the presence of a large excess of CO_2 (Fig. 7A). In harmony with this feature, the amount of carbon produced at 723 K (25.4 μmol/g) significantly exceeded that formed at 748 and 773 K (Fig. 7B).

The kinetic orders were calculated from the logarithmic plots of the various rates versus the volume percentage of the reactant of interest. The reaction temperature was 773 K, and the CO_2/C_2H_6 ratio was 6. The orders with respect to ethane were 0.42 and 0.64 for the formation of carbon monoxide and hydrogen, respectively. The order with respect to carbon dioxide was 0.18 for carbon monoxide formation and 0.34 for hydrogen evolution. From the temperature dependence of the rates of hydrogen and carbon monoxide production, the apparent activation energies were determined. We obtained 55.5 kJ/mol for H_2 production and 43.4 kJ/mol for CO formation.

4. DISCUSSION

4.1. Interaction of Ethane with Supported Rh

Before interpreting the data obtained for supported Rh we deal briefly with the nature of the adsorption of ethane on ZSM-5 support. Following the absorption and subsequent evacuation of ethane at 146–186 K we found relatively intense absorption bands at 2969, 2940, 2918, 2881, 1445, and 1371 cm^{-1} (Fig. 1A). These adsorption bands correspond well to those of molecularly adsorbed ethane: their assignments are presented in Table 1. Upon warming up the adsorbed layer ethane desorbed completely at and above 206 K without leaving any absorption bands. This suggests that ethane bonds weakly and reversibly on the ZSM-5 surfaces used as a support in the present study. (A more extended interaction occurs between ethane and ZSM-5 above 773 K, which involves dehydrogenation and even aromatization (16, 35, 36).) The same characteritics were observed for Rh/ZSM-5 at 146–200 K, indicating that ethane adsorbs mainly on ZSM-5 support.

The situation was completely different when the adsorpion of ethane was performed on Rh/ZSM-5 at 300 K. In this case new spectral features appeared at 1342, 2800, and 2879 cm^{-1} (Table 1). The 1342 cm^{-1} band, which was by far the most intense one, was detected at a temperature as low as 206 K. All these vibration modes have been observed following the adsorption of ethylene on different faces of Rh and on supported metals (37–41), which were attributed to the vibration of adsorbed ethylidyne. Furthermore, it was reported that ethylidyne decomposes on Rh(111) above 420 K. The resulting species are predominantly of type C_2H, although the presence of some CH surface species, implying C–C bond breaking, was also envisaged (37, 38). On the basis of similar spectral features, we may assume that the ethylidyne species is also produced by the strong interaction of ethane with reduced Rh cluster on ZSM-5, very likely through the transient formation of di-σ-bonded ethylene. The most intense vibrations of di-σ-ethylene are at 1420 and 2915 cm^{-1}. The fact that we could not detect these vibrations at any temperature after ethane adsorption suggests that the lifetime of adsorbed ethylene is very short; i.e., its transformation into ethylidyne occurs immediately after its production. The formation of ethylidyne from adsorbed ethane is not restricted to Rh/ZSM-5, as we observed intense bands of this species on Rh/Al_2O_3 and Rh/SiO_2 (42). De La Cruz and Sheppard (43) detected the prominent absorptions bands of ethylidyne following ethane adsorption on Pt/SiO_2 at 300 K. The absorptions from adsorbed ethylidyne weakened at 523 K and simultaneously new absorptions from gas phase methane were identified (43).

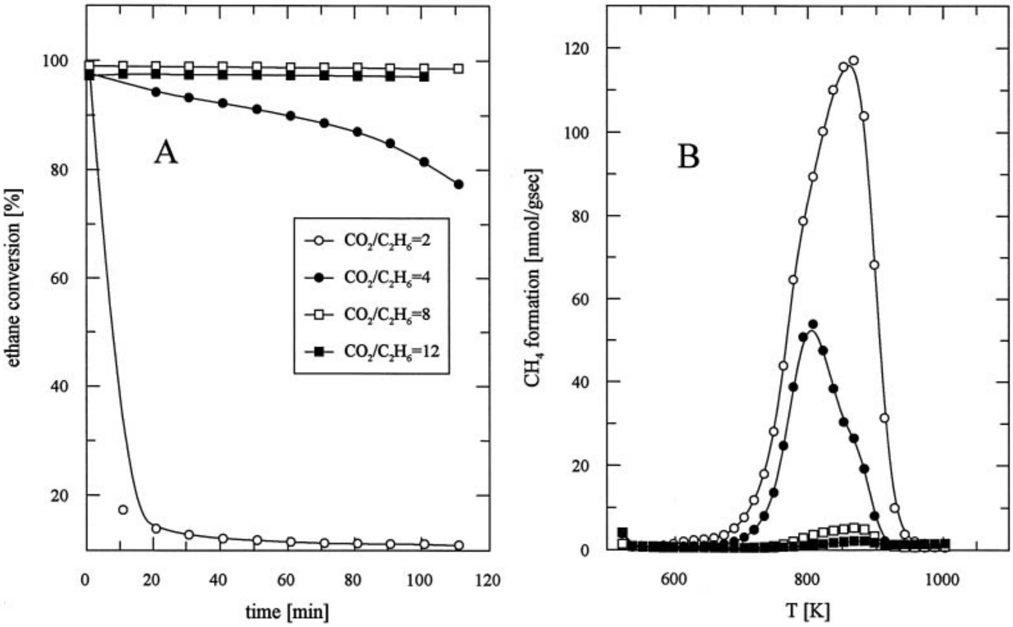

FIG. 6. Effects of CO_2/C_2H_6 ratio on (A) the conversion of ethane at 773 K and (B) the hydrogenation of surface carbon (TPR) formed by the reaction in 120 min.

TPR measurements confirmed the FTIR results and disclosed more details on the surface processes. In harmony with the IR results, no strongly adsorbed ethane was detected on the ZSM-5 used in this work. Activated adsorption of ethane occurred in the presence of Rh. As a result of the decomposition of adsorbed compounds, CH_4 and H_2 were released (Fig. 2). Their amounts increased with the increase in adsorption temperature of ethane from 373 to 623 K. TPR spectra also revealed a high temperature peak for H_2 ($T_p = 830$–900 K), when ethane was contacted with the catalyst at 523–623 K. This is very likely due to the decomposition of CH_x species remaining on the catalyst

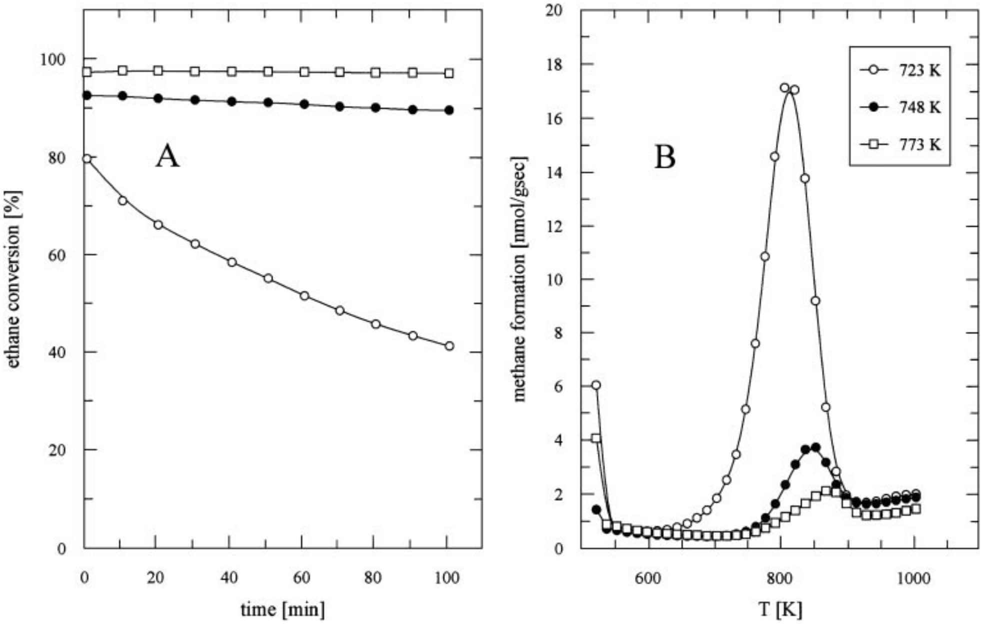

FIG. 7. Effects of temperature on (A) the conversion of ethane in the reaction mixture containing 5.2% C_2H_6 and 67% CO_2 and (B) the hydrogenation surface carbon producted on Rh/ZSM-5.

after the decomposition of ethylidyne. We can not exclude, however, the possibility that some of the CH_x fragments migrating from the Rh onto the ZSM-5 surface exhibit higher thermal stability than on the Rh clusters.

4.2. *Decomposition of Ethane in a Flow System*

Rh/ZSM-5 proved to be an active catalyst for the decomposition of ethane. At lower temperatures, 523–573 K, methane and propane were formed indicating the occurrence of the reaction

$$2C_2H_6 = C_3H_8 + CH_4.$$

Simultaneously, the dehydrogenation of ethane may have also proceeded,

$$C_2H_6 = C_2H_4 + H_2,$$

but no ethyene was released into gas phase. This occurred, however, from 623 K, and more predominantly from 673 K. At the same time, the formation of benzene and, at 723–773 K, toluene was also observed. As on Rh/SiO_2 no or a much lesser amount of aromatic compounds was identified, we are safe to conclude that these compounds are produced on the ZSM-5 support. The source of the benzene is very likely the ethylene which, through oligomerization and aromatization steps, readily transforms into benzene on the acidic sites of ZSM-5 (8–16, 29, 30).

Similar to the decomposition of methane on the same catalysts, the rate of the decomposition of ethane reduced to low levels after 10–15 min of contact time. This is, no doubt, due to the deposition of the carbonaceous species which blocks the rhodium. As complete cessation of the reaction was not attained even after several hours, we assume the migration of the carbonaceous species from the Rh onto the support.

4.3. *Reaction of Surface Carbon Produced by Ethane Decomposition*

As was shown first by our laboratory the reactivity of surface carbon and the distribution of carbon species on Rh catalysts depends on the temperature of carbon formation (44, 45). Following the dissociation of CO at low temperature, we distinguished three forms of carbon: (i) the highly reactive carbidic form (α), which can be hydrogenated even below 350 K; (ii) a less reactive amorphous layer (β), with a peak temperature of hydrogenation of $\sim$500 K; and (iii) the relatively inactive graphitic form (γ), which reacts with hydrogen only above 650 K. Recently, it was shown that these carbon species are produced by the low-temperature decomposition of methane on supported Rh (3–7). The more reactive carbon was missing, however, when it was produced by the high-temperature decomposition of CH_4, very likely due to its transformation into a less reactive form.

In the present work we are mainly concerned with the reaction of carbon species (produced at higher temperatures) with different gases. The results presented in Figs. 4A and 4B clearly show that the reactivity of carbon produced by ethane decomposition also depends on the temperature of its formation. Besides, the divergent reactivity is exhibited not only in its hydrogenation but also in its reactions with O_2 and CO_2. The T_p value for oxidation shifted from 520 to 683 K, when the temperature of the production of carbon was increased from 623 to 773 K. Much greater increases occurred in the peak temperature of the reaction of carbon with H_2 and CO_2 (Figs. 4A and 4B).

The reactivity order of the gases, $O_2 > H_2 > CO_2$, qualitatively corresponds to the ease of the activation of these gases over Rh. Whereas O_2 and H_2 can be activated readily on Rh even below room temperature, the activation of CO_2 may occur only above 400 K (46–50). This may suggest that the primary step of the reaction of C in these processes is the activation of reacting partners on the Rh.

4.4. *Interaction of Ethane with CO_2*

From the extensive study of the interaction of CO_2 with Rh(111) and supported Rh it appeared unambiguously that CO_2 interacts only weakly with Rh, and the dissociation of CO_2 proceeded only at elevated temperatures (46–50). When the dissociation of CO_2 was observed at a lower temperature, 300–423 K, it was caused either by boron impurity (50) or by the presence of adsorbed H atoms remaining on the supported Rh after reduction (46–50). Recently, we found that adsorbed CH_3 species can also induce the dissociation of CO_2 (51). The lowering of the dissociation temperature for CO_2 observed for the CH_4–CO_2 mixture on the Rh catalysts was partly attributed to the interaction and reaction between adsorbed CH_3 and CO_2 (6, 28).

An enhancement of the dissociation of CO_2 was experienced in the presence of ethane too, but its extent was much less than that measured at the coadsorption of the $CH_4 + CO_2$ gas mixture on the same catalyst (28). The intensity of this band was always higher then that obtained in the absence of ethane. Note that the analysis of IR spectra of coadsorbed species taken at different temperatures provided no sign for the formation of a surface complex between the two compounds. It should also be pointed out that we observed no CO formation when C_2H_6 and CO_2 were coadsorbed in the temperature range 300–673 K on the ZSM-5 support, which indicates that the activation of C_2H_6 is required for the C_2H_6–CO_2 interaction.

With regard to the enhancement of the dissociation of CO_2 we may assume that the adsorbed species formed in the surface decomposition of ethane, by interacting with the CO_2, promote the transformation of the CO_2 from the linear structure to any of the bent structures (50),

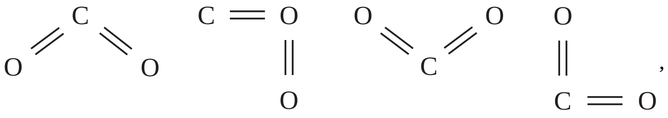

in which the reactivity of CO_2 is greatly increased. The fact that the promotion of the CO_2 dissociation is less compared to that observed in the $CH_4 + CO_2$ system may be because the ethylidyne, the detectable surface species in the interaction of ethane with Rh, is not an effective scavanger for the oxygen of CO_2.

We may also take into account the transitory formation of the formate-like species.

$$H_{(a)} + CO_{2(g)} = HCOO_{(a)}.$$

The formate species, however, is very unstable on Rh; it decomposes to CO_2 and H_2 even below 300 K (52, 53). Alternatively, it migrates onto the support where it can be accumulated and stabilized. This can not occur, however, for Rh/SiO_2, as the formate species does not exist on silica (46, 47, 53).

4.5. *Reaction of C_2H_6 and CO_2 at High Temperature*

It was interesting to see that adding CO_2 (5–10%) to C_2H_6 did not influence the decomposition of ethane at 523–623 K; the rate, the product distribution, and the deactivation remained practically the same. Above 623 K, the reaction between CO_2 and ethane (and its decomposition products) became more pronounced; as a result the formation of hydrocarbons gradually decreased and the production of H_2 and CO came into prominence. Kinetic measurements were performed in the temperature range 700–773 K. In contrast with the $CH_4 + CO_2$ reaction on the same Rh catalyst, a significant deactivation of the catalyst occurred at the stoichiometric composition due to carbon deposition. The rate of deactivation, however, diminished with the increase in the reaction temperature. The use of a large excess of CO_2 also lowered or even eliminated the deactivation.

As was expected, the rate of the CO and H_2 production increased with the space velocity, which lowered the probability of the back reactions. Taking into account all the observations mentioned we illustrate the dry reforming of ethane below.

Decomposition of ethane.

$$
\begin{aligned}
C_2H_{6(g)} &= C_2H_{6(a)}\\
C_2H_{6(a)} &= C_2H_{5(a)} + H_{(a)}\\
C_2H_{5(a)} &= \text{di-}\sigma\text{-}C_2H_{4(a)} + H_{(a)}\\
\text{di-}\sigma\text{-}C_2H_{4(a)} &= C\cdot CH_{3(a)} + H_{(a)}\\
2C\cdot CH_{3(a)} &= 2CH_{(a)} + CH_{4(g)} + H_{2(g)} + C_{(a)}\\
CH_{(a)} &= C_{(a)} + H_{(a)}
\end{aligned}
$$

Reactions with CO_2.

$$
\begin{aligned}
CO_{2(g)} &= CO_{2(a)}\\
CO_{2(a)} &= CO_{(a)} + O_{(a)}\\
CO_{2(a)} + H_{(a)} &= CO_{(a)} + OH_{(a)}\\
H_{(a)} + CO_{2(g)} &= HCOO_{(a)}\\
HCOO_{(a)} &= CO_{(a)} + OH_{(a)}\\
2OH_{(a)} &= H_2O + O_{(a)}\\
CH_{x(a)} + CO_{2(g)} &= CH_xO_{(a)} + CO_{(a)}\\
CH_{x(a)} + O_{(a)} &= CH_xO_{(a)}\\
CH_xO_{(a)} &= CO_{(g)} + xH_{(g)}\\
CO_{(a)} &= CO_{(g)}\\
2H_{(a)} &= H_{2(g)}\\
C_{(a)} + CO_{2(g)} &= 2CO_{(g)}
\end{aligned}
$$

4.6. *Comparison of $CH_4 + CO_2$ and $C_2H_6 + CO_2$ Reactions*

Supported Rh is an effective catalyst for both processes. The reaction of ethane with CO_2 on Rh/ZSM-5 proceeds by a factor of 5 faster than that of $CH_4 + CO_2$ under exactly the same experimental conditions. This may be attributed to the easier activation of the C–H bond in C_2H_6. On the other hand, however, while no or very little carbon deposition occurs in the $CH_4 + CO_2$ reaction over Rh, this is more pronounced for the $C_2H_6 + CO_2$ reaction. As a result, the rate of deactivation is much higher. In our previous work we assumed that the lack of carbon deposition on Rh is due to the facile reaction between CH_x fragments (CH_3 and CH_2) and CO_2 (6). In other words these CH_x fragments react with CO_2 before decomposing to carbon. If we accept this explanation then we may come to the conclusion that in the decomposition of ethane different CH_x species are formed, which is actually the case. The primary product of C_2H_6 dissociation is C_2H_5, which through the formation of C_2H_4 gives a less reactive ethylidyne species (see Section 4.4).

Alternatively, a reaction between carbon and CO_2 has to be assumed to explain the lack of carbon deposition:

$$C + CO_2 = 2CO.$$

In this case, however, it is not easy to explain why the deactivation is so pronounced for the $C_2H_6 + CO_2$ reaction compared to the $CH_4 + CO_2$ process, as carbon formed at the same temperature should exhibit the same reactivity with CO_2. Therefore we consider this reaction route less likely.

ACKNOWLEDGMENTS

This work was supported by the Hungarian Academy of Sciences and by OTKA No. 2038. A loan of $RhCl_3$ from Johnson-Matthey is gratefully acknowledged.

REFERENCES

1. Bibby, D. M., Chang, C. D., Howe, R. F., and Yurchak, S. (Eds.), “Methane Conversion: Studies on Surface Science and Catalysis,” Vol. 36. Elsevier, Amsterdam, 1998.
2. Lunsford, J. H., *in* “Proceedings, 10th International Congress on Catalysis,” (L. Guczi, F. Solymosi, and P. Tétényi, Eds.), p. 103. Elsevier, Amsterdam, 1993.
3. van Santen, R. A., de Koster, A., and Koerts, T., *Catal. Lett.* **7**, 1 (1990).
4. Koerts, T., Deelen, M. J. A. G., and van Santen, R. A., *J. Catal.* **138**, 101 (1992).
5. Solymosi, F., Erdõhelyi, A., and Cserényi, J., *Catal. Lett.* **16**, 399 (1992).
6. Erdõhelyi, A., Cserényi, J., and Solymosi, F., *J. Catal.* **141**, 287 (1993).
7. Solymosi, F., and Cserényi, J., *Catal. Lett.* **34**, 343 (1995).
8. Wang, L., Tao, L., Xie, M., Xu, G., Huang, J., and Xu, Y., *Catal. Lett.* **21**, 35 (1993).
9. Xu, Y., Wang, L., Xie, M., and Gou, X., *Catal. Lett.* **30**, 135 (1995).
10. Solymosi, F., Erdõhelyi, A., and Szöke, A., *Catal. Lett.* **32**, 43 (1995).
11. Solymosi, F., and Szöke, A., *Catal. Lett.* **39**, 157 (1996).
12. Solymosi, F., Cserényi, J., Szöke, A., Bánsági, T., and Oszkó, A., *J. Catal.* **165**, 150 (1997).
13. Lunsford, J. H., Rosynek, M. P., and Wang, D. W., *Stud. Surf. Sci. Catal.* **107**, 257 (1997).
14. Wang, D., Lunsford, J. H., and Rosynek, M. P., *Top. Catal.* **3(4)**, 299 (1996).
15. Wang, D., Lunsford, J. H., and Rosynek, M. P., *J. Catal.* **169**, 347 (1997).
16. Solymosi, F., and Szöke, A., *Appl. Catal. A* **166**, 225 (1998).
17. Rostrup-Nielsen, J. R., *Stud. Surf. Sci. Catal.* **36**, 73 (1988).
18. Rostrup-Nielsen, J. R., Aasberg-Petersen, K., and Schoubye, P. S., *Stud. Surf. Sci. Catal.* **107**, 473 (1997).
19. Zhang, Z. L., and Verykios, X. E., *Catal. Today* **21**, 589 (1994).
20. Choudhary, V. R., Uphade, B. S., and Mamman, A. S., *Appl. Catal. A.* **168**, 33 (1998).
21. Solymosi, F., Kutsán, Gy., and Erdõhelyi, A., *Catal. Lett.* **11**, 149 (1991).
22. Mark, M. F., and Maier, W. F., *J. Catal.* **164**, 122 (1996).
23. Zhang, Z. L., Tsipouriari, V. A., Efstathiou, A. M., and Verykios, X. E., *J. Catal.* **158**, 51 (1996); Tsipouriari, V. A., Efstathiou, A. M., and Verykios, X. E., *J. Catal.* **158**, 64 (1996).
24. Bhat, R. N., and Sachtler, W. M. H., *Appl. Catal. A* **150**, 279 (1997).
25. Nakamura, J., Aikawa, K., Sato, K., and Uchijima, T., *Catal. Lett.* **25**, 265 (1994).
26. Ferreira-Aparicio, P., Guerrero-Ruiz, A., and Rodriguez-Ramos, I., *Appl. Catal. A* **170**, 177 (1998).
27. Sigl, M., Bradford, M. C. J., Knözinger, H., and Vannice, M. A., *Top. Catal.*, in press.
28. Szöke, A., Ph.D. thesis, A. József University, Szeged; Solymosi, F., Szõke, A., and Egri, L., *Top. Catal.*, in press.
29. Rossner, F., Klepel, O., and Hagen, A., *Stud. Surf. Sci. Catal.* **107**, 517 (1997).
30. Liu, Y., Xue, J., Liu, X., Hou, R., and Li, S., *Stud. Surf. Sci. Catal.* **119**, 593 (1998).
31. Rostrup-Nielsen, J. R., *J. Catal.* **31**, 173 (1973).
32. Rostrup-Nielsen, J. R., *J. Catal.* **33**, 184 (1974).
33. Wisnosky, M. G., Eggers, D. F., Fredrickson, L. R., and Decius, J. C., *J. Chem. Soc. Faraday Trans. 1* **79**, 3505 (1983).
34. Kondo, J., Domen, K., Maruya, K., and Onishi, T., *J. Chem. Soc.* **86**(21), 3665 (1990).
35. Guisnet, M., Gnep, N. S., and Alario, F., *Appl. Catal.* **89**, 1 (1992).
36. Schulz, P., and Baerns, M., *Appl. Catal.* **78**, 15 (1991).
37. Dubois, L. H., Castner, D. G., and Somorjai, G. A., *J. Chem. Phys.* **72**, 5234 (1980).
38. Somorjai, G. A., van Hove, M. A., and Bent, B. E., *J. Phys. Chem.* **92**, 973 (1988).
39. Mohsin, S. B., Trenary, M., and Robota, H. J., *J. Phys. Chem.* **95**, 6657 (1991).
40. Soma, Y., *J. Catal.* **59**, 239 (1979).
41. Beebe, T. P., Jr., and Yates, J. T., Jr., *J. Phys. Chem.* **91**, 254 (1987).
42. Ovári, L., Ph.D. thesis, A. József University, Szeged.
43. De La Cruz, C., and Sheppard, N., *J. Catal.* **127**, 445 (1991).
44. Solymosi, F., and Erdõhelyi, A., *Surf. Sci.* **110**, L630 (1981).
45. Erdõhelyi, A., and Solymosi, F., *J. Catal.* **84**, 446 (1984).
46. Solymosi, F., Erdõhelyi, A., and Kocsis, M., *J. Catal.* **65**, 2351 (1980); Solymosi, F., Bánsági, T., and Erdõhelyi, A., *J. Chem. Soc. Faraday Trans. 1* **77**, 2645 (1981).
47. Solymosi, F., Erdõhelyi, A., and Bánsági, T., *J. Catal.* **68**, 371 (1981).
48. Henderson, M. A., and Worley, S. D., *Surf. Sci.* **149**, 392 (1985).
49. Henderson, M. A., and Worley, S. D., *J. Phys. Chem.* **89**, 392 (1985).
50. Solymosi, F., *J. Mol. Catal.* **65**, 337 (1991).
51. Raskó, J., and Solymosi, F., *Catal. Lett.* **46**, 153 (1997).
52. Solymosi, F., and Kiss, J., *J. Catal.* **81**, 95 (1983).
53. Solymosi, F., and Erdõhelyi, A., *J. Catal.* **91**, 327 (1985).